◼ Fluorescent Probes

Na+ Selective Fluorescent Tools Based on Fluorescence Intensity Enhancements, Lifetime Changes, and on a Ratiometric Response

Thomas Schwarze,*[a] Janine Riemer,[a] Holger Müller,[a] Leonard John,[b] Hans-Jürgen Holdt,[a] and Pablo Wessig*[b]

Abstract: Over the years, we developed highly selective fluorescent probes for K+ in water, which show K+-induced fluorescence intensity enhancements, lifetime changes, or a ratiometric behavior at two emission wavelengths (cf. Scheme 1, **K1–K4**). In this paper, we introduce selective fluorescent probes for Na+ in water, which also show Na+ induced signal changes, which are analyzed by diverse fluorescence techniques. Initially, we synthesized the fluorescent probes **2**, **4**, **5**, **6** and **10** for a fluorescence analysis by intensity enhancements at one wavelength by varying the Na+ responsive ionophore unit and the fluorophore moiety to adjust different K_d values for an intra- or extracellular Na+ analysis. Thus, we found that **2**, **4** and **5** are Na+ selective fluorescent tools, which are able to measure physiologically important Na+ levels at wavelengths higher than 500 nm. Secondly, we developed the fluorescent probes **7** and **8** to analyze precise Na+ levels by fluorescence lifetime changes. Herein, only **8** ($K_d = 106$ mm) is a capable fluorescent tool to measure Na+ levels in blood samples by lifetime changes. Finally, the fluorescent probe **9** was designed to show a Na+ induced ratiometric fluorescence behavior at two emission wavelengths. As desired, **9** ($K_d = 78$ mm) showed a ratiometric fluorescence response towards Na+ ions and is a suitable tool to measure physiologically relevant Na+ levels by the intensity change of two emission wavelengths at 404 nm and 492 nm.

Introduction

Na+ is a vital element in life science and plays a fundamental role in many biological processes, such as nerve conduction as well as muscle and heart contraction.[1a,b] Therefore, for the top analyte Na+ an exact determination method is required to provide true conclusions about the role of Na+ in these biological processes. Further, to get reliable data about Na+ levels in vivo the Na+ selectivity of the fluorescent probe and the sensitivity of the analytical method is of fundamental importance. Fluorescent probes consisting of an ionophore (ion binding moiety) and a fluorophore (signaling unit), so-called fluoroionophores, are common in use for the sensitive fluorometric analysis of Na+ in vitro and in vivo. Most of the reported Na+ fluoroionophores show moderate Na+ induced fluorescence enhancements (FE) at a single wavelength,[2a–h] which is based on an off switching of a photoinduced electron transfer (PET) by Na+.[3a–d] For the analysis of Na+ levels in vivo, the measurement at a single wavelength requires a costly calibration and is very sensitive to cellular dye concentration changes. However, a more precise method to quantify Na+ levels in vivo is based on Na+ fluoroionophores, which show a ratiometric emission behavior or a change of the fluorescence lifetime. Currently, only a small number of ratiometric[4a–d] and fluorescence lifetime[5a–d] probes for Na+ were developed.

Further, the dissociation constant (K_d) of the Na+-fluoroionophore-complex must fit to the extracellular (100 mm–150 mm) or intracellular (5 mm–30 mm) Na+ concentration range to track physiologically important Na+ levels in vivo. A specific challenge is the Na+/K+ selectivity of the fluoroionophore, because K+ is the competitive cation in animal cells and it shows an extracellular (1 mm–10 mm K+) and intracellular (100 mm–150 mm K+) concentration range, which is contrary to Na+. Furthermore, in blood samples the Na+ level ranges from 135 mm to 148 mm and the competitive K+ level from 3.5 mm to 5.3 mm. A broader Na+ concentration range is found in urine samples (114 mm–210 mm). Therefore, tailor-made selective Na+ fluoroionophores could be useful to analyze Na+ levels in blood and urine samples.

Recently, we synthesized by CuAAC reactions (CuAAC = CuI-catalyzed 1,3-dipolar azide alkyne cycloaddition reaction)[6a,b] highly K+ selective fluorescent probes for the exclusive determination of K+ by fluorescence enhancements,[7a–d] fluores-
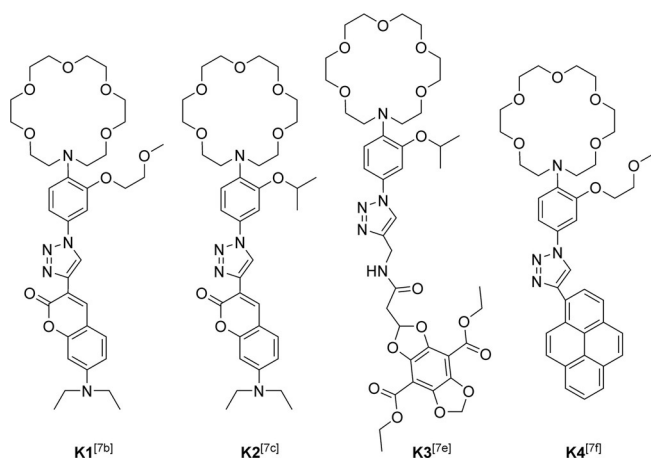
[a] Dr. T. Schwarze, J. Riemer, H. Müller, Prof. Dr. H.-J. Holdt
Institut für Chemie, Anorganische Chemie
Universität Potsdam, Karl-Liebknecht-Str. 24–25, 14476 Golm (Germany)
E-mail: schwarth@uni-potsdam.de

[b] L. John, Prof. Dr. P. Wessig
Institut für Chemie, Bioorganische Chemie
Universität Potsdam, Karl-Liebknecht-Str. 24–25, 14476 Golm (Germany)
E-mail: wessig@uni-potsdam.de

⊡ Supporting information and the ORCID identification number(s) for the author(s) of this article can be found under:
https://doi.org/10.1002/chem.201902536.

cence lifetime changes[7e] and by a ratiometric behavior[7f] at two emission wavelengths in water (cf. Scheme 1, see highly K+ selective fluorescent probes **K1**-**K4**). Representatives for highly K+ selective PET fluoroionophores are **K1**[7b] and **K2**[7c] consisting of highly K+ selective building blocks the *N*-(*o*-2-methoxyethoxy)phenylaza-18-crown-6 in **K1** and the isopropoxy substituted *N*-phenylaza-18-crown-6 in **K2** and of a diethylaminocoumarin unit as a fluorophore in both **K1** and **K2**, respec-

tively. The PET fluoroionophore **K3**[7e] consisting of a [1,3]dioxolo[4,5-*f*][1,3]benzodioxole (DBD) fluorophore and of a highly K+ selective ionophore (cf. **K3** and **K2**). **K3** is an appropriate fluorescence lifetime probe to track extracellular K+ levels. A further K+ selective fluorescent probe is **K4**, which is based on a K+ induced state reversal in water and this results in a ratiometric fluorescence change at two emission wavelengths in the presence of K+.[7f] Further, we also developed Na+ selective PET-fluoroionophores **1**[5d] and **3**[8] for extracellular Na+ levels determination. Both consist of a *N*-(*o*-methoxyphenyl)aza-15-crown-5 unit and of a coumarin-derived fluorophore (cf. Scheme 2).

In this paper, we introduce a set of Na+ responsive fluorescent probes, which are capable to measure cellular Na+ levels by different fluorescence techniques. Na+ probes **1**–**6** and **10** are PET fluoroionophores to detect Na+ by a moderate FE at a single wavelength. The emission wavelength and quantum yield (φ_f) of the Na+ probes **1**–**6** and **10** depends mainly on the coumarin fluorophore. Therefore, the resulting Na+ induced FE is a result of the substituted coumarin moieties in position 6 and 8. In detail, a fixed alkylated amino group on the coumarin unit leads to a higher φ_f in polar solvents (cf. Scheme 2, fluorescent probe **4**, **5** and **6**).[9a,b] Thus, we synthesized probes **2**, **4**, **5**, **6** and **10** to get fluoroionophores with different φ_f and λ_{max}. Further, the ionophore moieties in **2**, **4** and **10** differ from each other, but all consist of an aza-15-crown-5 macrocycle to bind exclusively Na+ over K+. To improve the


Scheme 1. Highly K+/Na+ selective fluorescent probes **K1**-**K4**.[7b,c,e,f]
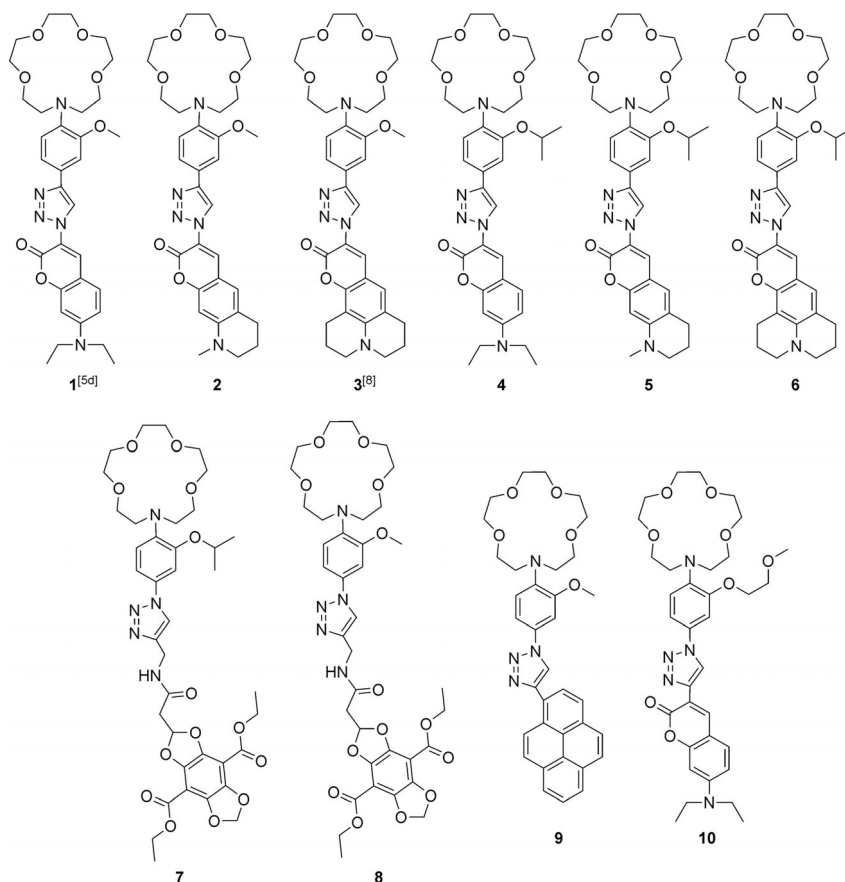
Scheme 2. Structures of the Na+ responsive fluorescent probes **1**–**10** studied.

Na$^+$ selectivity, we introduced in *ortho* position of the aniline unit an isopropoxy moiety (cf. **4**, **5** and **6**) or a 2-methoxyethoxy lariat ether (cf. **10**). Previously, this bulky substituents in *ortho* position showed an enhanced K$^+$ selectivity effect in combination with an aza-18-crown-6 moiety (cf. **K1** and **K2** in Scheme 1).[7b,c] Further, to design Na$^+$ selective probes, which show Na$^+$ induced fluorescence lifetime changes, we used a similar architecture as shown in compound **K3**. Herein, we exchanged the highly K$^+$ selective building block (cf. **K3**) by a *N*-(o-methoxyphenyl)aza-15-crown-5 moiety (cf. **8**) or by a *N*-(o-isopropoxyphenyl)aza-15-crown-5 unit (cf. **7**). Both consist of a DBD fluorophore, which exhibits a high quantum yield ($\varphi_f = \approx 0.60$) and an extraordinary fluorescence lifetime ($\tau_f = \approx 20$ ns) in water.[10] These probes **7** and **8** are also PET fluoroionophores, which show FEs at a single wavelength and moderate fluorescence lifetime changes in the presence of Na$^+$. Further, to obtain ratiometric fluorescent probes, we synthesized probe **9**, which consists of a Na$^+$ selective ionophore (*N*-(o-methoxyphenyl)aza-15-crown-5) and a pyrene fluorophore connected by a 1,2,3-triazole unit. We decided to construct the fluorescent probe **9** in a similar fashion, as the K$^+$ selective dye **K4**, to get a Na$^+$ induced ratiometric fluorescence behavior at two emission wavelengths. Overall, our ultimate goal is to develop highly Na$^+$/K$^+$ selective fluorescent tools to measure reliable Na$^+$ levels in vivo by diverse fluorescence techniques.

Results and Discussion

Syntheses of 1,2,3-triazol-1,4-diyl-fluoroionophores

To obtain the Na$^+$ responsive fluorescent probes **2**, **4**, **5**, **6**, **7**, **8**, **9** and **10** in a feasible number of synthetic steps (Scheme 3 and Scheme 4), we started the synthesis of the ionophore derivatives from commercially available 1-fluoro-2-alkoxy-4-nitrobenzene derivatives **14a** and **14b**, 1-fluoro-2-alkoxy-4-formylbenzene derivatives **11a** and **11b** and 1-bromo-2-(2-methoxyethoxy)-4-nitrobenzene **14c** (Scheme 3). The *N*-(4-formyl-2-alkoxyphenyl)aza-15-crown-5 ether [R=Me (**12a**) and *i*Pr (**12b**)] derivatives were prepared in yields up to 44% from the reaction of 1-aza-15-crown-5 with an excess of the corresponding 1-fluoro-2-alkoxy-4-formylbenzene derivatives **11a** and **11b** (cf. Scheme 3). The transformation of the aldehyde group in **12a** and **12b** to a terminal ethynyl unit (cf. Scheme 3. *N*-(4-Ethynyl-2-alkoxyphenyl)aza-15-crown-5 ether [R=Me (**13a**) and *i*Pr (**13b**)]) was achieved with the reagent dimethyl-1-diazo-2-oxopropylphosphonate.[11] Further, in a similar synthetic procedure compared to **12a** and **12b**, we synthesized the *N*-(4-nitro-2-alkoxyphenyl)aza-15-crown-5 ether [R=Me (**15a**) and *i*Pr (**15b**)] derivatives in yields up to 96% from the reaction of 1-aza-15-crown-5 with an excess of the corresponding 1-fluoro-2-alkoxy-4-nitrobenzene **14a** and **14b** derivatives. The *N*-(4-nitro-2-(2-methoxyethoxy)phenyl)aza-15-crown-5 (**15c**) was
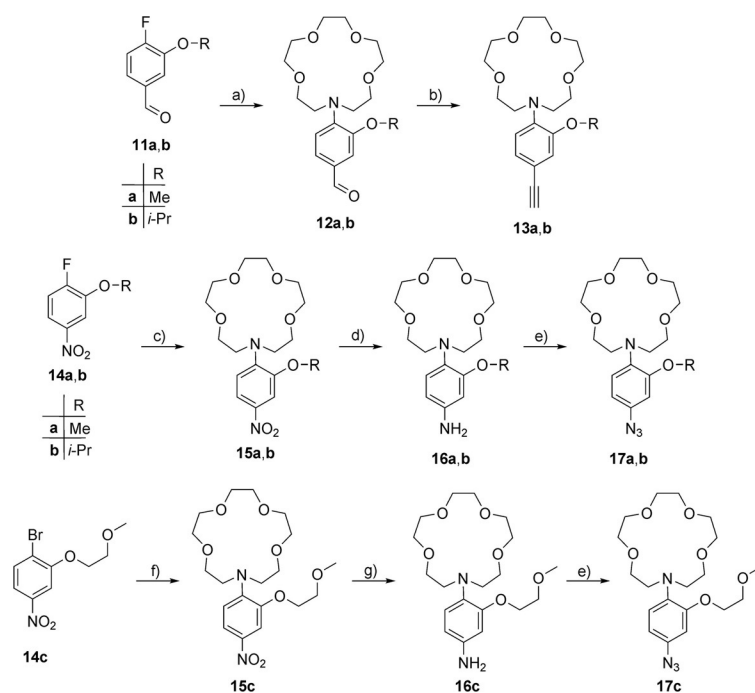
Scheme 3. Syntheses of the alkynyl- and azido-substituted Na$^+$ responsive ionophores **13a**, **13b**, **17a**, **17b** and **17c**: a) 1-aza-15-crown-5, K$_2$CO$_3$, DMF, reflux; b) dimethyl-1-diazo-2-oxopropylphosphonate,[11] K$_2$CO$_3$, MeOH, RT; c) 1-aza-15-crown-5, Cs$_2$CO$_3$, DMF, reflux; d) SnCl$_2\cdot$2H$_2$O, HCl, ethylacetate, 40°C; e) NaNO$_2$, NaN$_3$, HCl, 0°C to RT; f) Pd(OAc)$_2$, PPh$_3$, NaOC(CH$_3$)$_3$, 1-aza-15-crown-5, toluene; g) H$_2$, 10% Pd/C, MeOH, 50 bar, RT.

prepared by a Pd^{II}-catalyzed coupling reaction of 1-bromo-2-(2-methoxyethoxy)-4-nitrobenzene **14c** with the 1-aza-15-crown-5 (Buchwald-Hartwig amination). A subsequent reduction of the nitro group in **15a** and **15b** by SnCl$_2\cdot$2H$_2$O in HCl or by H$_2$ on Pd/C for **15c** gave the *N*-(4-amino-2-alkoxyphenyl)aza-15-crown-5 ether derivatives **16a**, **16b** and **16c** and a subsequent diazotization of the amino compounds and reaction of the resulting diazonium salt with sodium azide afforded the azides **17a**, **17b** and **17c** [R=Me (**17a**), *i*Pr (**17b**) and EtOMe (**17c**)]. The final synthesis of the 1,2,3-triazol-1,4-diyl-fluoroionophores **2**, **4**, **5**, **6**, **7**, **8**, **9** and **10** were realized by CuAAC reactions of the alkynyl functionalized ionophores **13a** and **13b** with the corresponding azido functionalized coumarin derivatives to yield **2**, **4**, **5** and **6**, respectively and of the azido functionalized ionophores **17a**, **17b** and **17c** with the alkynyl substituted DBD, pyrene or coumarin fluorophores (cf. Scheme 4). Overall, we synthesized fluoroionophores **2**, **4**, **5**, **6**, **7**, **8**, **9** and **10** in a sequence of only three or four subsequent synthetic steps (see Scheme 3 and 4).

Spectroscopic properties of 1–6 and 10 in the presence of Na$^+$ and K$^+$ in water

The UV/Vis absorption spectra of **2**, **4**, **5**, **6** and **10** exhibit two charge transfer (CT) bands in a H$_2$O/DMSO (99/1, v/v) mixture (see Figures S1a-S1d and S1f), as already found for the Na$^+$ responsive fluoroionophores **1** and **3**.[5d,8] The long-wavelength CT absorptions for the coumarin-derived derivatives are centered at 425 nm for **2**, at 427 nm for **4** and at 420 nm for **10**,
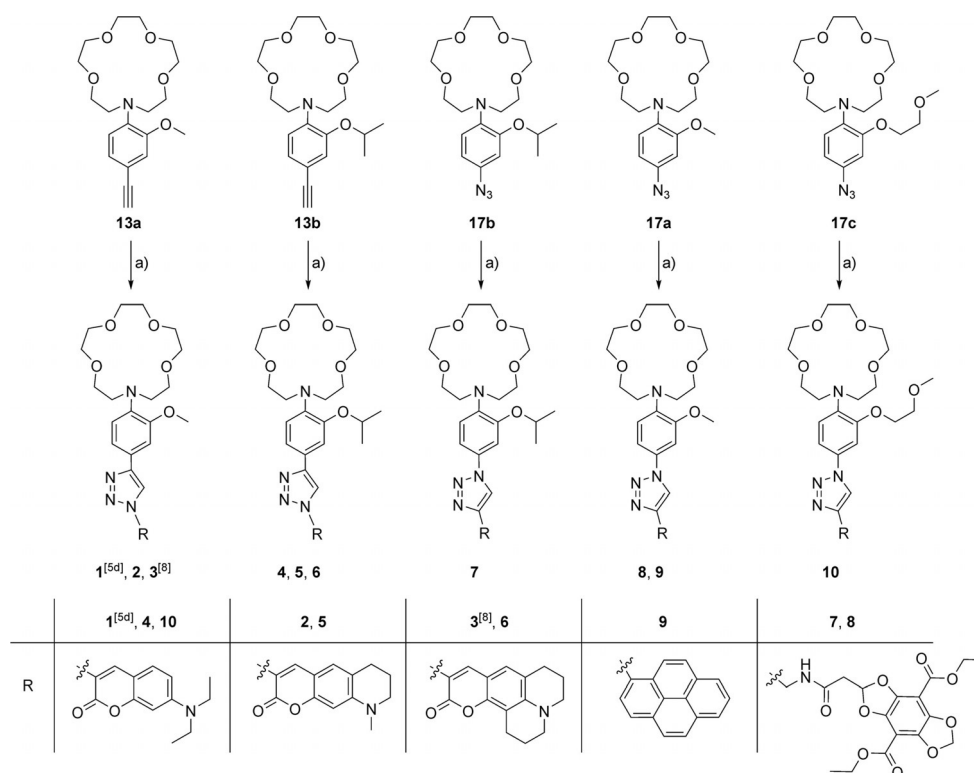
Scheme 4. Synthetic route of the studied Na$^+$ responsive fluorescent probes **1–10**: a) CuSO$_4$/Na ascorbate, THF/H$_2$O, 60 °C, for **4** the 3-azido-7-diethylamino-coumarin,[12a] for **2** and **5** the 3-azido-9-methyl-6,7,8,9-tetrahydro-2H-pyrano[3,2-g]quinolin-2-one,[13] for **6** the 10-azido-2,3,6,7-tetrahydro-1 H,5 H,11H-pyrano[2,3-f]pyrido[3,2,1-ij]quinolin-11-one,[12a] for **7** and **8** the diethyl 2-[2-oxo-2-(prop-2-yn-1-ylamino)ethyl]benzo[1,2-d:4,5-d′]bis[1,3]dioxole-4,8-dicarboxylate,[10] for **9** the commercial available 1-ethynylpyrene, and for **10** the 3-ethynyl-7-diethylcoumarin,[12b] respectively.

which is comparable to the coumarin CT absorption at 422 nm for **1**. A slightly red-shifted long wavelength CT is found for **5** at 430 nm and for **6** at 435 nm. For **2, 4, 5, 6** and **10**, the second CT absorption band, which is typical for π-conjugated anilino-1,2,3-triazol-1,4-diyl-fluoroionophores,[8] can be found for **2, 4, 5, 6** and **10** at around 300 nm corresponding to a CT from the nitrogen lone pair of the aromatic ring (donor) to the 1,2,3-triazole acceptor unit. Further, we studied the influence of Na$^+$ and K$^+$ towards the UV/Vis absorption of **2, 4, 5, 6** and **10** in a H$_2$O/DMSO (v/v, 99/1) mixture. For **2, 4, 5, 6** and **10**, we found no change of the long-wavelength absorption in the presence of Na$^+$ or K$^+$ (cf. Figures S1 a–d and S1 e). Here, the complexation of Na$^+$ or K$^+$ with **2, 4, 5, 6** and **10** can be seen from the CT absorption at around 300 nm (see Figures S1 a–d and S1 f). We observed for **2, 4, 5, 6** and **10** a Na$^+$ induced decrease of the CT band at around 300 nm and a smaller K$^+$ induced change of this CT band (cf. Figure S1 a–d and S1 f). Thus, the complexed Na$^+$ decreases the donor ability of the anilino unit in **2, 4, 5, 6** and **10**, which leads to a decrease of the CT absorption band at around 300 nm.

Further, the fluorescence spectra of **1** and **4** showed emissions centered at 500 nm, for **2** and **5** emissions at 502 nm and for **3** and **6** emissions at around 520 nm (cf. Table 1). Thus, the respective triazole substituted coumarin derivative adjusted λ_{max}. Herein, we found for probes **2, 4, 5, 6** and **10** different quantum yields φ_f (cf. Table 1). Overall, the φ_f of **1–6** and **10** were lower than that of the pure coumarin fluorophore. The

low φ_f of probes **2, 4, 5, 6** and **10** (cf. Table 1) suggests that a photoinduced electron transfer (PET) takes place, which quenches the fluorescence, as already observed for the Na$^+$-responsive 1,2,3-triazol-fluoroionophores **1** and **3**.[5d,8]

To validate the Na$^+$/K$^+$ selectivity of **2, 4, 5, 6** and **10**, we investigated the influence of Na$^+$ and K$^+$ on the fluorescence intensity of **2, 4, 5, 6** and **10**. Initially, we performed titration experiments with **2, 4, 5, 6** and **10** only in the presence of Na$^+$. Thus, we observed for **2, 4, 5, 6** and **10** a FE in the presence of Na$^+$ (see Figure 1 for **2**, Figures S3 a–S6 a and S10 a). In summary, Figure 2 shows the titration curves of **2, 4, 5, 6** and **10**+Na$^+$ at λ_{max} nm. The fluorescent probe **2** showed the highest Na$^+$ induced FE by a factor of 8.1. However, we observed smaller Na$^+$ induced FE factors for **4** (FEF=2.4), **5** (FEF=2.9), **6** (FEF=3.1) and **10** (FEF=2.5). The maximal FE was reached for **2, 4, 5, 6** and **10** at a Na$^+$ concentration of around 750 mм (see Figure 2). Further, we found for **2, 4, 5, 6** and **10**+Na$^+$ enhanced φ_f values (cf. Table 1). The Na$^+$ induced FEs of **1–6** and **10** can be explained by an off switching of the PET quenching process by Na$^+$, as already observed for several π-conjugated anilino-1,2,3-triazol-1,4-diyl-fluoroionophores for Na$^+$ and K$^+$ (cf. **1, 3** and **K1** and **K2**).[5d,7b,c,8] In a further step, we measured the fluorescence response towards K$^+$ and found a smaller influence on the fluorescence intensity for **2, 4, 5, 6** and **10**+K$^+$. We observed for **2**+1000 mм K$^+$ a FEF of 1.8, for **4**+1000 mм K$^+$ a FEF of 1.2, for **5**+1000 mм K$^+$ a FEF of 1.1, for **6**+1000 mм K$^+$ a FEF of 1.3 and for **10**+1000 mм K$^+$ a FEF of

Table 1. Photophysical properties of **1–10** in water.[a]					
	λ_{abs} [nm]	λ_f [nm]	φ_f[b]	FEF[c]	K_d^{Na+}[d] [mM]
1	422	500	0.009	–	–
1 + Na⁺	422	500	0.048	5.0	117
1 + K⁺	422	500	0.017	1.5	276
2	425	502	0.038	–	–
2 + Na⁺	425	502	0.297	8.1	87
2 + K⁺	425	502	0.070	1.8	190
3	440	517	0.025	–	–
3 + Na⁺	440	517	0.275	10.9	48
3 + K⁺	440	517	0.067	2.7	68
4	427	500	0.012	–	–
4 + Na⁺	427	500	0.028	2.4	195
4 + K⁺	427	500	0.015	1.2	–[e]
5	430	502	0.030	–	–
5 + Na⁺	430	502	0.090	2.9	241
5 + K⁺	430	502	0.035	1.1	–[e]
6	435	520	0.025	–	–
6 + Na⁺	435	520	0.076	3.1	264
6 + K⁺	435	520	0.035	1.3	–[e]
7	414	516	0.041	–	–
7 + Na⁺	414	516	0.128	3.1	>300
7 + K⁺	414	516	0.066	1.6	–[e]
8	415	517	0.028	–	–
8 + Na⁺	415	517	0.126	4.5	106
8 + K⁺	415	517	0.045	1.6	–[e]
9	285, 370	388, 404, 492	0.035	–	–
9 + Na⁺	285, 358	388, 404	0.033	–	78
9 + K⁺	285, 370	388, 404, 492	0.034	–	–[e]
10	420	494	0.043	–	–
10 + Na⁺	420	494	0.106	2.5	89
10 + K⁺	420	494	0.082	1.9	106

[a] All data were measured in a H₂O/DMSO (v/v, 99/1) mixture in the absence and presence of 1 M NaCl or 1 M KCl, respectively. [b] Fluorescence quantum yield, (±15)%. [c] Fluorescence enhancement factor, [$FEF = I/I_0$], (±0.2). [d] Dissociation constants K_d for Na⁺-and K⁺-complexes. [e] K_d values for K⁺-complexes could not be determined, caused by the low K⁺ induced intensity changes.
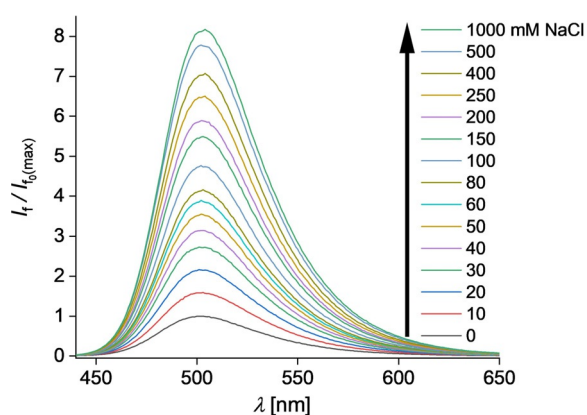

Figure 2. Fluorescence enhancement factors of **2** (black), **4** (red), **5** (blue), **6** (green) and **10** (purple) in Tris (10 mM, pH 7.2) buffered H₂O/DMSO mixtures (99/1, v/v) in the presence of various Na⁺ concentrations.

Figure 1. Fluorescence intensity changes of **2** ($c = 10^{-5}$ M, $\lambda_{exc} = 420$ nm) in Tris (10 mM, pH 7.2) buffered H₂O/DMSO mixtures (99/1, v/v) in the presence of various Na⁺ concentrations.

1.9. Herein, in this series, we found for **2**, **4**, **5** and **6** a moderate Na⁺/K⁺ selectivity, but for **10** a very poor Na⁺/K⁺ selectivity. We assume that the poor Na⁺/K⁺ selectivity of **10** is caused by the effect that the two O-atoms of the 2-methoxyethoxy group also complexes to K⁺. Herein, K⁺ fits not exactly into
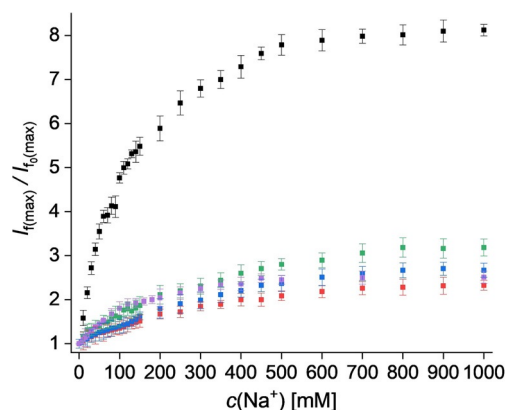
the cavity of the aza-15-crown-5 moiety and the resulting K⁺ complex is stabilized by the two O-atoms of the 2-methoxyethoxy lariat group. Thus, we found for **10** + K⁺ compared to the K_d value of the methoxy substituted fluorescent probe **1** + K⁺ (276 mM, cf. Table 1) a reduced K_d value of 106 mM.

Dissociation constants (K_d) of fluorescent probes **2** + Na⁺, **4** + Na⁺ **5** + Na⁺, **6** + Na⁺ and **10** + Na⁺ were calculated from plots of fluorescence intensities of **2**, **4**, **5**, **6** and **10** versus Na⁺ ion concentrations.[13] In all cases, we observed a 1:1 complexation, indicated by the slopes (≈1) of the plots.[13] For **2** + Na⁺, **4** + Na⁺, **5** + Na⁺, **6** + Na⁺ and **10** + Na⁺, we found K_d values of 87 mM, 195 mM, 241 mM, 264 mM and 89 mM, respectively (cf. Table 1). Herein, **4**, **5** and **6**, consisting of the N-(o-isopropoxy-phenyl)aza-15-crown-5 ionophore, showed the highest K_d values in this series. The fluorescent probes **1**, **2** and **3**, which are equipped with the N-(o-methoxyphenyl)aza-15-crown-5 ionophore, show lower K_d values (see Table 1). We conclude that the isopropoxy substituent sterically hampers the Na⁺ complexation. Herein, **2** and **10** formed the strongest Na⁺ complexes, but also complexes to K⁺ (cf. Table 1, FEF (**2** + K⁺) = 1.8, K_d = 190 mM; FEF (**10** + K⁺) = 1.9), K_d = 106 mM). The 2-methoxyethoxy substituted ionophore in **10** showed a very poor Na⁺/K⁺ selectivity and is not suitable to measure selectively Na⁺ levels in the presence of K⁺. Further, we tested the suitability of **2**, **4** and **5** to measure Na⁺ in the presence of physiological relevant K⁺ levels. Thus, we prepared different Na⁺ solutions, containing 10 mM KCl to simulate the extracellular K⁺ background. Under these conditions, the K_d values of **2** + Na⁺ (92 mM), **4** + Na⁺ (235 mM) and **5** + Na⁺ (239 mM) are slightly influenced by 10 mM KCl (see Figures S3 c, S4 c and S5 c). Further, the high Na⁺/K⁺ selectivity can be also seen from the FE factors of **2** + Na⁺ (FEF = 8.0), **4** + Na⁺ (FEF = 2.2) and **5** + Na⁺ (FEF = 2.6) in the presence of 10 mM KCl (cf. Figures S3 d, S4 d and S5 d). Thus, the performance of **2**, **4** and **5** is only slightly influenced by these K⁺ levels. Particularly, the fluorescent probes **4** and **5**, which are equipped by the N-(o-isopropoxyphenyl)aza-15-crown-5 ionophore are approbate fluorescent tools to measure Na⁺ levels in blood samples.

The Na$^+$-selectivity of fluorescent probes **2**, **4**, **5** and **6** was verified by titration experiments with other metal ions. Particularly, we focused on biological important cations such as K$^+$, Ca^{2+}, Mg^{2+}, Li$^+$, Fe^{2+}, Fe^{3+}, Ni^{2+}, Cu^{2+} and Zn^{2+} at their physiological concentrations (see Figure S3h for **2**, Figure S4g for **4**, Figure S51 g for **5** and Figure S6d for **6**). These cations show only negligible effects on the fluorescence of **2**, **4**, **5** and **6**. Moreover, **2**, **4**, **5** and **6** recognized Na$^+$ even in the co-presence of these metal ions, as shown in Figures S3h, S4g, S5g and S6d. Further, to verify the pH sensitivity of **2**, **4**, **5** and **6**, we measured the fluorescence at different pH values.[13] Thus, we found only minor effects towards the sensitivity of **2**, **4**, **5** and **6** at various concentrations of Na$^+$ ions within the pH range from 6.8 to 8.8 (see Figures S3i, S4h, S5h and S6e). Therefore, **2**, **4**, **5** and **6** were capable fluorescent probes to determine selective biological important Na$^+$ levels.

Spectroscopic properties of 7 and 8 in the presence of Na$^+$ and K$^+$ in water

The UV/Vis absorption spectra of **7** and **8** in a H$_2$O/DMSO mixture (99/1, v/v) show also two absorptions, which are composed of the DBD fluorophore and the triazole substituted *N*-phenylaza-15-crown-5 ionophore (Figures S2a and b). The long-wavelength absorption in the spectra of **7** and **8**, centered at 414 nm and 415 nm, (cf. Table 1) belongs to a n–π* absorption of the DBD moiety.[7e, 10] The short-wavelength absorption in the spectra of **7** and **8**, centered at around 300 nm, corresponds to a CT from the nitrogen lone pair of the anilino moiety (electron donor) to the 1,2,3-triazole electron acceptor, as already observed for **K3**.[7e] Herein, the Na$^+$ coordination can be also seen from a Na$^+$ induced decrease of the CT band at around 300 nm (Figure S2a and b). In contrast to Na$^+$, K$^+$ only slightly changes this CT absorption band, demonstrating the high Na$^+$/K$^+$ selectivity of **7** and **8**. Further, the n–π* absorption of the DBD moiety is unaffected by Na$^+$ or K$^+$ (cf. Table 1, Figures S2a and b).

Further, the fluorescence spectra of **7** and **8** show similar emissions centered at 516 nm and 517 nm and similar quantum yields φ_F (φ_F (**7**) = 0.041, φ_F (**8**) = 0.028, cf. Table 1), but the φ_F values are lower than the φ_F value of the pure DBD fluorophore (φ_F = 0.63[10]). Therefore, a PET process in **7** and **8** quenches the fluorescence, as already shown for fluorescent probe **K3**. Due to the underlying PET process in **7** and **8**, the observed fluorescence kinetics are complex. The fluorescence decay curves at λ_{em} = 447 nm (λ_{ex} = 415 nm) for **7** and **8** could be reasonably well fitted using tri-exponential decay kinetics (τ_1 = 4.8 ns (58%), τ_2 = 0.5 ns (21%) and τ_3 = 23.1 ns (21%) for **7**, τ_1 = 5.1 ns (48%), τ_2 = 0.5 ns (22%) and τ_3 = 23.9 ns (30%) for **8**).

In a next step, we investigated the influence of Na$^+$ and K$^+$ on the fluorescence intensity and decay time of **7** and **8**. Further, we observed a FE of **7** and **8** with increasing Na$^+$ or K$^+$ concentrations at λ_{max} (for **8**+Na$^+$ see Figure 3), which is typical for PET fluoroionophores. The fluorescent probe **8** exhibits a higher Na$^+$ induced FE by a factor of 4.5, compared to **7** (FEF = 3.1, see Figure 4), but both fluorescent probes show a very similar FEF in the presence of K$^+$ (FEF = 1.6, cf. Table 1).
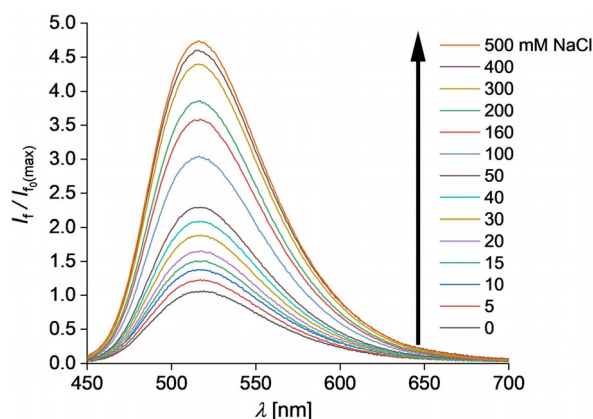

Figure 3. Fluorescence intensity changes of **8** ($c = 10^{-5}$ M, λ_{exc} = 415 nm) in Tris (10 mM, pH 7.2) buffered H$_2$O/DMSO mixtures (99/1, v/v) in the presence of various Na$^+$ concentrations.
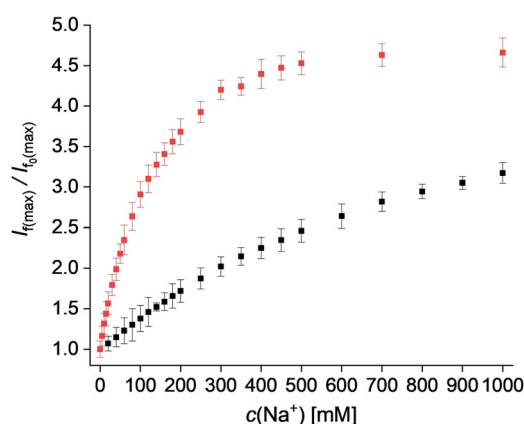

Figure 4. Fluorescence enhancement factors of **7** (black) and **8** (red) in Tris (10 mM, pH 7.2) buffered H$_2$O/DMSO mixtures (99/1, v/v) in the presence of various Na$^+$ concentrations.

The maximal FE for **8** was reached in the presence of around 750 mM Na$^+$, but for **7**+Na$^+$ we observed even in the presence of 1000 mM NaCl an enhancement of the fluorescence intensity (cf. Figure 4). The φ_f values of **7** and **8** were also enhanced in the presence of Na$^+$ and K$^+$ (cf. Table 1).

Further, we also observed for **7** and **8** in the presence of Na$^+$ (1000 mM) tri-exponential decay kinetics with similar decay times and proportions yielding decay times of τ_1 = 5.9 ns (64%), τ_2 = 1.1 ns (6%) and τ_3 = 14.8 ns (30%) for **7** and of τ_1 = 8.8 ns (83%), τ_2 = 0.3 ns (2%) and τ_3 = 17.6 ns (15%) for **8** (cf. Figure 5a and b). We also investigated the influence of competing K$^+$ ions towards **7** and **8**. The fluorescence decay times of **7** and **8** are slightly affected by 1000 mM KCl (τ_1 = 5.1 ns (63%), τ_2 = 0.9 ns (20%) and τ_3 = 20.7 ns (17%) for **7**, τ_1 = 5.0 ns (60%), τ_2 = 1.3 ns (19%) and τ_3 = 24.2 ns (21%) for **8**; cf. Figures 5a and b).

Interestingly for **7** and **8**, we observed during complexation of Na$^+$, that τ_1 and the fraction of τ_1 increases but τ_3 decreases and τ_2 and the fraction of τ_2 are only slightly affected by Na$^+$ (cf. Figures S11b,c, S12b and c). As a consequence, the averaged fluorescence decay time ($\tau_{f(av)}$) decreases for **7** from
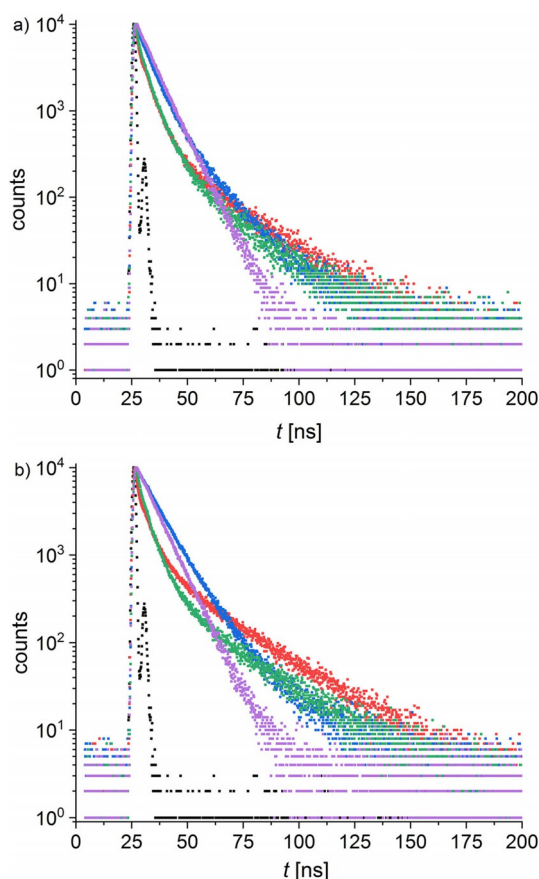
Figure 5. Fluorescence decay time changes of a) **7** ($c = 10^{-5}$ M, $\lambda_{exc} = 447$ nm, red) and b) **8** ($c = 10^{-5}$ M, $\lambda_{exc} = 447$ nm, red) in a Tris (10 mM, pH 7.2) buffered H_2O/DMSO (v/v, 99/1) mixture in the presence of 1 M NaCl (blue), 1 M KCl (green) and 0.1 M HCl (purple) and the instrumental response (black).

16.3 ns to 10.6 ns and for **8** from 18.9 ns to 11.1 ns, respectively (cf. Figure 6). We assume, that the underlying PET process is interrupted by Na^+ and this can be seen from the τ_1 value. The decay time τ_1 is enhanced and although the fraction of τ_1 is increased by Na^+, as normally observed for PET fluoroionophores, which show Na^+ induced fluorescence intensity and
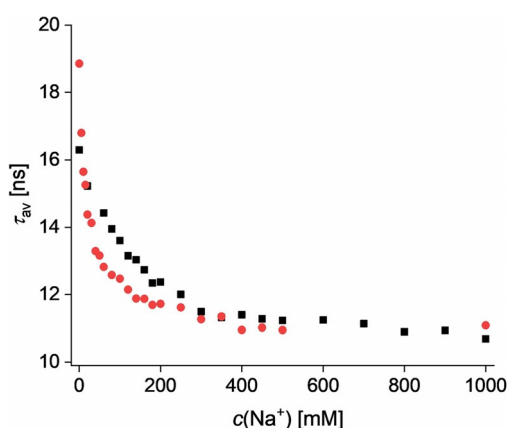

Figure 6. Averaged fluorescence decay time changes of **7** ($c = 10^{-5}$ M, $\lambda_{exc} = 447$ nm, black) and **8** ($c = 10^{-5}$ M, $\lambda_{exc} = 447$ nm, red) in the presence of various Na^+ concentrations.

decay time enhancements. Further, for complete blocking of the PET process in **7** and **8**, we added to **7** and **8** a 0.1 M HCl solution to protonate the N-atom of the anilino unit. Therefore, we observed bi-exponential decay kinetics for both fluoroionophores. For **7** + H^+ values of 3.8 ns (14 %) and 8.1 ns (86 %) and for **8** + H^+ values of 4.0 ns (7 %) and 8.1 ns (93 %). The decay time value of 8.1 ns become a more dominating amount. Consequently, the $\tau_{f(av)}$ of **7** + H^+ and **8** + H^+ is also reduced from 16.3 ns to 7.8 ns for **7** + H^+ and from 18.9 ns to 7.9 ns for **8** + H^+ (cf. Figures 5 a and b), compared to the unprotonated compounds **7** and **8**. Noticeable, the long decay time component τ_3 disappears by H^+. Further, we assume that conformational changes of the DBD fluorophore within **7** and **8** are responsible for the decay time τ_3. This process is non-radiative and is hampered by Na^+ and H^+. Overall, we observed for **7** + Na^+ and **8** + Na^+ an enhanced quantum yield φ_f, but a reduced $\tau_{f(av)}$, whereby τ_1 is increased by an off switching of the fluorescence quenching PET process.

Dissociation constants (K_d) of fluorescent probe **7** + Na^+ and **8** + Na^+ were also calculated from plots of fluorescence intensities versus Na^+ ion concentrations.[13] The K_d value of **8** + Na^+ is 106 mM, which fits to physiologically important Na^+ levels. Further, for **7** + Na^+ a precise determination of the K_d value based on intensity was not possible caused by the continuous signal change in the presence of Na^+ ions (cf. Figure 4). A preliminary analysis showed for **7** + Na^+ a K_d value of > 300 mM.[13] Herein, the isopropoxy substituted ionophore in **7** also hampers the Na^+ complexation (cf. **4** + Na^+) and we observed a higher K_d value as compared to **8** + Na^+ (106 mM).

Further, we verified the Na^+-selectivity of fluorescent probes **7** and **8** by titration experiments with other metal ions (K^+, Ca^{2+}, Mg^{2+}, Li^+, Fe^{2+}, Fe^{3+}, Ni^{2+}, Cu^{2+} and Zn^{2+}, see Figure S7 e for **7** and Figure S8 e for **8**). Herein, we found only negligible effects on the performance of **7** and **8**. Moreover, **7** and **8** showed within the pH range from 6.8 to 8.8 only minor effects towards the fluorescence signal (see Figures S3 i, S4 h, S5 h and S6 e). Therefore, **7** and **8** were also capable fluorescent probes to determine selective biological important Na^+ levels.

Spectroscopic properties of 9 in the presence of Na^+ and K^+ in water

The UV/Vis absorption spectrum of **9** in Tris buffered (10 mM, pH of 7.2) H_2O/DMSO mixtures 99/1 (v/v) show superimpositions of CT bands and the typical polycyclic aromatic absorption bands (cf. Figure S1 e). **9** exhibits two CT bands at around 285 nm and 370 nm. The short-wavelength CT absorption at around 285 nm corresponds to a CT from the nitrogen lone pair of the aromatic ring (donor) to the 1,2,3-triazole acceptor unit, which is also found for a set of π-conjugated anilino-1,2,3-triazol-1,4-diyl-fluoroionophores.[5d, 7a,b] The CT band at around 370 nm is superimposed by the pyrenyl absorption bands and belongs to a CT from the anilinotriazole donor moiety to the pyrenyl acceptor unit, as already shown for probe **K4**.[7f] Further, we observed for **9** + Na^+ a slightly blue-

shifted and decreased CT band at around 370 nm and a slightly reduced CT band at around 285 nm (cf. Figure S1 e).

The fluorescence spectrum of **9** ($\lambda_{ex} = 345$ nm) in Tris buffered (10 mм, pH of 7.2) H$_2$O/DMSO mixtures of 99/1 (v/v) showed a dual emission behavior (cf. Figure 7). We observed
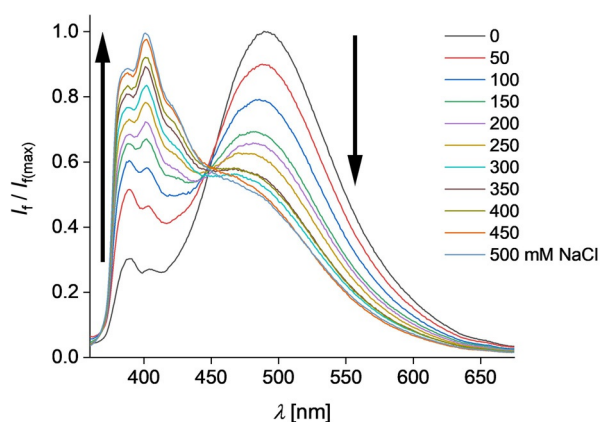

Figure 7. Fluorescence intensity changes of **9** ($c = 10^{-5}$ м, $\lambda_{exc} = 345$ nm) in Tris (10 mм, pH 7.2) buffered H$_2$O/DMSO mixtures (99/1, v/v) in the presence of various Na$^+$ concentrations.

for **9** in the range from 370 nm to 440 nm the typical pyrene emission from the LE state and a broad emission peaked at 492 nm, which corresponds to a fluorescent CT state, as also observed for **K4**.[7f] Thus, **9** has a fluorescent CT state (S1) and a lower fluorescent LE state (S2) in a H$_2$O/DMSO mixture of 99/1 (v/v). The φ_f value of **9** is 0.035 (Table 1).

Further, we investigated the influence of Na$^+$ and K$^+$ on the fluorescence intensity of **9**. Herein, the fluorescence signal of **9** + Na$^+$ showed remarkable intensity changes at 404 nm and 492 nm (cf. Figure 7 and Figure 8). Na$^+$ reduces the fluorescence intensity of the CT state at 492 nm by a factor of 2.1 to a concentration of around 450 mм NaCl. However, Na$^+$ enhances the fluorescence intensity ($FEF = 3.6$, see Figure 7) of the LE state at 404 nm. Thus, **9** showed a dual fluorescence emission behavior in the presence of Na$^+$. Overall, we observed similar φ_f values for **9** + 1000 mм NaCl ($\varphi_f = 0.033$) and
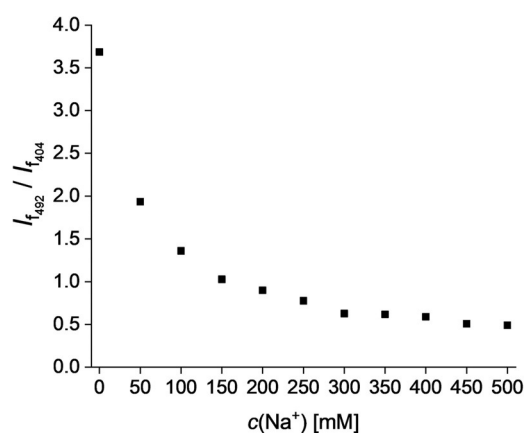

Figure 8. Titration curve of **9** ($c = 10^{-5}$ м) in the presence of various Na$^+$ concentrations.

for **9** + 1000 mм KCl ($\varphi_f = 0.034$, Table 1), but the high Na$^+$/K$^+$ selectivity of **9** can be seen from Figure S9 d. K$^+$ only slightly affected the emission behavior of **9** (cf. Figure S9 d). Thus, the presence of K$^+$ has a negligible effect on the performance of **9** under simulated physiological conditions. The dissociation constant was calculated from plots of fluorescence intensities versus Na$^+$ concentrations.[13] The K_d of **9** + Na$^+$ is 78 mм. We assume, that the ratiometric emission behavior of **9** + Na$^+$ is caused by a Na$^+$ induced state reversal in water. Further, **9** operates in the presence of Na$^+$ in a similar mechanistic way as found for **K4** + K$^+$.[7f]

We also verified the Na$^+$-selectivity of fluorescent probe **9** by titration experiments with other metal ions (K$^+$, Ca^{2+}, Mg^{2+}, Li$^+$, Fe^{2+}, Fe^{3+}, Ni^{2+}, Cu^{2+} and Zn^{2+}, see Figure S9 e) and checked the sensitivity of **9** within the pH range from 6.8 to 8.8 (see Figure S9 f). Herein, we found only negligible effects on the performance of **9** towards these cations and these pH values.

Conclusions

In summary, we synthesized via CuAAC reactions Na$^+$ responsive fluorescent tools **2**, **4**, **5**, **6**, **7**, **8**, **9** and **10**, which operate by diverse photophysical processes. Fluorescent probes **2**, **4**, **5**, **6** and **10** show a Na$^+$ induced off switching of the fluorescence quenching PET mechanism and as a result a FE at a single wavelength (>500 nm) in water. The Na$^+$/K$^+$ selectivity of **2**, **4** and **5** is probate to measure physiologically important Na$^+$ levels. Particularly, fluorescent probe **2** + Na$^+$ shows the highest FE by a factor of 8.1 and a K_d value of 87 mм. The Na$^+$/K$^+$ selectivity and the Na$^+$ complex stability is influenced by the ionophore moiety. The N-(o-isopropoxyphenyl)aza-15-crown-5 moiety in **5** complexes weaker to Na$^+$ than the N-(o-methoxyphenyl)aza-15-crown-5 unit in **4**, caused by the steric hindrance of the bulky isopropoxy group. A similar influence on the ionophore moiety towards the K_d value is found for **7** + Na$^+$ ($K_d = >300$ mм) and **8** + Na$^+$ (106 mм). The fluorescent probes **7** and **8** show also a Na$^+$ induced off switching of the PET process. Further, **7** + Na$^+$ and **8** + Na$^+$ exhibit a FE at a single wavelength (>500 nm) and show reduced averaged fluorescence lifetimes from 16.3 ns to 10.6 ns for **7** + Na$^+$ and from 18.9 ns to 11.1 ns for **8** + Na$^+$. Fluorescent probe **8** is a suitable tool to detect biological important Na$^+$ levels by fluorescence lifetime changes in water. A further Na$^+$ selective fluorescent tool is probe **9**, which shows a Na$^+$ induced ratiometric fluorescence behavior at two emission wavelengths. For **9** + Na$^+$, we found at 492 nm a decrease of the CT band by a factor of 2.1 and an increase of the fluorescence intensity at 404 nm by a factor of 3.6. Herein, Na$^+$-induces a state reversal in water. As a rare example, **9** is a Na$^+$ selective and ratiometric fluorescent probe, which is able to detect biologically important Na$^+$ levels. Overall, we are able to measure physiologically relevant Na$^+$ levels by a FE at a single emission wavelength, by fluorescence lifetime changes and by the intensity change of two emission wavelengths. Currently in our lab, we synthesizing highly Ca^{2+} selective fluorescent probes based on

fluorescence intensity, lifetime changes and by a ratiometric response.

Experimental Section

General methods and reagents

All commercially available chemicals were used without further purification. Solvents were distilled prior use. ^{1}H and ^{13}C NMR spectra were recorded on 300 MHz or 500 MHz instruments, respectively. Data are reported as follows: chemical shifts in ppm (δ), multiplicity (s = singlet, d = doublet, t = triplet, dd = doublet of doublets, m = multiplet), integration, coupling constant (Hz). ESI spectra were recorded using a Micromass Q-TOF micro mass spectrometer in a positive electrospray mode. Column chromatography was performed with silica gel (Merck; silica gel 60 (0.04–0.063 mesh)).

Synthesis and characterization

General synthetic procedures for 12a and 12b: A mixture of 1-aza-15-crown-5 (1.25 g, 5.7 mmol), the corresponding 1-fluoro-2-alkoxy-4-formylbenzene derivatives **11a** or **11b** (cf. Scheme 3) (28.5 mmol) and K$_2$CO$_3$ (0.87 g, 6.27 mmol) in dry DMF (12 mL) was refluxed for 12 h. After cooling down to room temperature the residue was filtered off and the organic phase was concentrated in vacuo. The resulting residue was purified by column chromatography on silica using CHCl$_3$/CH$_3$OH (v/v, 99/1 to 95/5) as eluent mixtures to afford **12a** and **12b** as pale yellow oils.

***N*-(4-Formyl-2-methoxyphenyl)aza[15]crown-5 ether (12a):** Yield 44% (886 mg). Analytical data of **12a** can be found in Reference [2d].

***N*-(4-Formyl-2-isopropoxyphenyl)aza[15]crown-5 ether (12b):** Yield 32% (690 mg); ^{1}H NMR (CDCl$_3$, 300 MHz): δ = 9.71 (s, 1H), 7.34–7.28 (m, 2H), 7.25 (d, J = 1.6 Hz, 1H), 4.62 (dt, J = 12.1, 6.0 Hz, 1H), 3.72 (t, J = 5.7 Hz, 4H), 3.65–3.60 (m, 16H), 1.33 ppm (d, J = 6.0 Hz, 6H); ^{13}C NMR (CDCl$_3$, 75 MHz): δ = 190.3, 148.9, 147.0, 128.8, 126.3, 117.1, 113.0, 71.3, 70.6, 70.6, 70.6, 70.4, 53.6, 22.1 ppm; HRMS (EI): m/z calcd for C$_{20}$H$_{31}$NO$_6$: 381.2151 [M^+]; found: 381.2150.

General synthetic procedures for 13a and 13b: To a mixture of the corresponding aldehyde derivative **12a** or **12b** (1.81 mmol) and 500 mg (3.63 mmol) K$_2$CO$_3$ in 16 mL dry methanol was added 410 mg (2.12 mmol) dimethyl-1-diazo-2-oxopropylphosphonate.[11] This suspension was stirred for 10 hours at room temperature. After addition of 60 mL CHCl$_3$, the organic layer was extracted with water (10 mL), separated, dried with MgSO$_4$ and concentrated in vacuo. The resulting residue was purified by column chromatography on silica with CHCl$_3$/CH$_3$OH (v/v, 95/5) as an eluent mixture to afford **13a** or **13b** as pale yellow oils.

***N*-(4-Ethynyl-2-methoxyphenyl)aza[15]crown-5 ether (13a):** Yield 63% (398 mg). Analytical data of **13a** can be found in Reference [5d].

***N*-(4-Ethynyl-2-isopropoxyphenyl)aza[15]crown-5 ether (13b):** Yield 98% (670 mg); ^{1}H NMR (CDCl$_3$, 300 MHz): δ = 7.01 (dd, J = 8.2, 1.9 Hz, 1H), 6.92 (s, 1H), 6.90 (s, 1H), 4.53 (dt; J = 12.1, 6.1 Hz, 1H), 3.71–3.60 (m, 16H), 3.49 (t, J = 6.1 Hz, 4H), 2.98 (s, 1H), 1.32 ppm (d, J = 6.1 Hz, 6H); ^{13}C NMR (CDCl$_3$, 75 MHz): δ = 150.0, 142.8, 125.7, 120.1, 119.2, 114.2, 84.7, 75.5, 71.4, 70.9, 70.7, 70.6, 53.4, 22.3 ppm; HRMS (ESI): m/z calcd for C$_{21}$H$_{31}$NO$_5$+H$^+$: 378.2280 [M+H$^+$]; found: 378.2244.

General synthetic procedures for 15a and 15b: A mixture of 1-aza-15-crown-5 (840 mg, 3.82 mmol), the corresponding 1-fluoro-2-alkoxy-4-nitrobenzene derivatives **14a** or **14b** (cf. Scheme 3) (19.1 mmol) and Cs$_2$CO$_3$ (1.24 g, 3.82 mmol) in DMF (9 mL) was refluxed for 10 h. After cooling down to room temperature the residue was filtered off and the organic phase was concentrated in vacuo. The resulting residue was purified by column chromatography on silica using CHCl$_3$/CH$_3$OH (v/v, 99/1 to 95/5) as eluent mixtures to afford **15a** and **15b** as yellow oils.

***N*-(4-Nitro-2-methoxyphenyl)aza[15]crown-5 ether (15a):** Yield 96% (1.36 g). Analytical data of **15a** can be found in Reference [14].

***N*-(4-Nitro-2-isopropoxyphenyl)aza[15]crown-5 ether (15b):** Yield 92% (1.4 g); ^{1}H NMR (CDCl$_3$, 300 MHz): δ = 7.77 (dd, J = 9.0, 2.5 Hz, 1H), 7.64 (d, J = 2.3 Hz, 1H), 6.90 (d, J = 7.9 Hz, 1H), 4.67–4.59 (m, 1H), 3.73–3.61 (m, 20H), 1.37 ppm (d, J = 6.0 Hz, 6H); ^{13}C NMR (CDCl$_3$, 75 MHz): δ = 147.4, 146.6, 139.6, 118.1, 116.0, 109.4, 71.2, 71.1, 70.5, 70.4, 70.0, 53.9, 21.9 ppm; HRMS (EI): m/z calcd for C$_{19}$H$_{30}$N$_2$O$_7$: 398.2035 [M^+]; found: 398.2054.

General synthetic procedures for 16a and 16b: The nitro compound **15a** or **15b** (4.84 mmol) was added to a solution of SnCl$_2$·2H$_2$O (1.34 g, 5.96 mmol) in conc. HCl (3 mL) and ethylacetate (10 mL) and stirred for 2 h at 40°C. After that, H$_2$O (10 mL) was added and the resulting solution was stirred for 24 h at 40°C. Afterwards, the solution was adjusted to a pH value of 8 with NaOH (40%) and extracted with CH$_2$Cl$_2$ (100 mL), separated, dried with MgSO$_4$ and concentrated in vacuo. The resulting residue was purified by column chromatography on silica with CHCl$_3$/CH$_3$OH (v/v, 95/5) as an eluent mixture to afford **16a** or **16b** as brownish oils.

***N*-(4-Amino-2-methoxyphenyl)aza[15]crown-5 ether (16a):** Yield 75% (1.24 g). Analytical data of **16a** can be found in Reference [14].

***N*-(4-Amino-2-isopropoxyphenyl)aza[15]crown-5 ether (16b):** Yield 60% (1.07 g); ^{1}H NMR (CDCl$_3$, 300 MHz): δ = 6.95 (d, J = 8.8 Hz, 1H), 6.24 (d, J = 2.2 Hz, 1H), 6.18 (dd, J = 8.2, 2.3 Hz, 1H), 4.54–4.46 (m, 1H), 3.71–3.54 (m, 16H), 3.30 (t, J = 5.2 Hz, 4H), 1.31 ppm (d, J = 6.0 Hz, 6H); ^{13}C NMR (CDCl$_3$, 126 MHz): δ = 162.7, 153.5, 112.1, 107.7, 107.1, 102.9, 70.8, 70.5, 70.2, 69.9, 54.5, 22.3 ppm; HRMS (EI): m/z calcd for C$_{19}$H$_{32}$N$_2$O$_5$: 368.2311 [M^+]; found: 368.2302.

Synthetic procedure for 15c: A mixture of 1-bromo-2-(2-methoxyethoxy)-4-nitrobenzene (736 mg, 2.67 mmol), PPh$_3$ (42 mg, 0.16 mmol), Pd(OAc)$_2$ (18 mg, 0.08 mmol), sodium *tert*-butoxid (333 mg, 3.47 mmol) and 1-aza-15-crown-5 (702 mg, 3.2 mmol) in dry toluene (15 mL) was refluxed for 24 h under an argon atmosphere. After that, CH$_2$Cl$_2$ (50 mL) was added and the catalyst was removed by filtration through a bed of Celite. The solvent was removed in vacuo and the resulting residue was purified by column chromatography on silica with CHCl$_3$/CH$_3$OH (v/v, 95/5) as an eluent mixture to afford **15c** as a yellow oil.

***N*-(4-Nitro-2-ethoxymethoxyphenyl)aza[15]crown-5 ether (15c):** Yield 52% (573 mg); ^{1}H NMR (CDCl$_3$, 300 MHz): δ = 7.73 (dd, J = 9.1, 2.5 Hz, 1H), 7.57 (d, J = 2.5 Hz, 1H), 6.79 (d, J = 9.1 Hz, 1H), 4.11–4.04 (m, 2H), 3.74–3.28 ppm (m, 25H); ^{13}C NMR (CDCl$_3$, 75 MHz): δ = 148.0, 145.9, 138.7, 118.5, 114.8, 108.0, 70.8, 70.4, 70.1, 70.1, 69.7, 67.7, 58.6, 53.7 ppm; HRMS (ESI): m/z calcd for C$_{19}$H$_{30}$N$_2$O$_8$+H$^+$: 415.4630 [M+H$^+$]; found: 415.2353.

Synthetic procedure for 16c: 10% Pd/C (60 mg) was added to a solution of **15c** (575 mg, 1.4 mmol) in dry MeOH (50 mL). The mixture was hydrogenated in an autoclave for 24 h at 50 bar. The catalyst was removed by filtration through a bed of Celite and the solvent was removed in vacuo to yield **16c** as a light yellow oil.

***N*-(4-Amino-2-ethoxymethoxyphenyl)aza[15]crown-5 ether (16c):** Yield 79% (426 mg). Caution! **22** quickly decomposed if exposed

to air at room temperature, thereby showing a color change to purple. HRMS (EI): m/z calcd for $C_{19}H_{32}N_2O_6$: 384.2260 $[M^+]$; found: 384.2262.

General synthetic procedures for 17a, 17b and 17c: To a solution of the corresponding amino compound **16a**, **16b** or **16c** (cf. Scheme 3) (2.9 mmol) in 4 M HCl (20 mL) was cooled to 0 °C. Then, a solution of $NaNO_2$ (200 mg, 2.9 mmol) in water (10 mL) was slowly added and the mixture was stirred at 0 °C for 10 min. Further, a solution of NaN_3 (283 mg, 4.4 mmol) in water (10 mL) was added at 0 °C and the mixture was stirred for 14 h at RT, neutralized with K_2CO_3, and extracted with $CHCl_3$ (3×50 mL). The organic layers were combined, dried over $MgSO_4$, concentrated in vacuo, and the residue was purified by column chromatography on silica gel ($CHCl_3$/MeOH, 95/5 v/v) to give compounds **17a**, **17b** and **17c** as brown oils.

***N*-(4-Azido-2-methoxyphenyl)aza[15]crown-5 ether (17a):** Yield: 78% (829 mg); Analytical data of **17a** can be found in Reference [5d].

***N*-(4-Azido-2-isopropoxyphenyl)aza[15]crown-5 ether (17b):** Yield 80% (920 mg); ^1H NMR (CDCl$_3$, 500 MHz): $\delta = 7.05$ (d, $J = 8.5$ Hz, 1 H), 6.55 (dd, $J = 8.5$, 2.5 Hz, 1 H), 6.45 (d, $J = 2.5$ Hz, 1 H), 4.55–4.49 (m, 1 H), 3.69–3.61 (m, 16 H), 3.39 (t, $J = 6.0$ Hz, 4 H), 1.32 ppm (d, $J = 6.0$ Hz, 6 H); ^{13}C NMR (CDCl$_3$, 125 MHz): $\delta = 152.2$, 138.7, 133.7, 122.8, 110.9, 106.4, 71.1, 70.7, 70.5, 70.4, 53.5, 22.2 ppm; HRMS (EI): m/z calcd for $C_{19}H_{30}N_4O_5$: 394.2216 $[M^+]$; found: 394.2222.

***N*-(4-Azido-2-ethoxymethoxyphenyl)aza[15]crown-5 ether (17c):** Yield: 12% (143 mg); Caution! **23** quickly decomposed if exposed to air at room temperature, thereby showing a color change to dark brown. HRMS (EI): m/z calcd for $C_{19}H_{30}N_4O_6$: 410.2165 $[M^+]$; found: 410.2170.

General CuACC procedure for 2, 4, 5 and 6: A mixture of the corresponding alkynyl substituted crown compound **13a** or **13b** (0.329 mmol) and the corresponding azidocoumarin derivative[12a] (cf. Scheme 4) (0.329 mmol), $CuSO_4 \cdot 5H_2O$ (4.1 mg) and sodium ascorbate (6.5 mg) in 9 mL THF/H_2O (v/v, 2/1) was stirred at 60 °C for 48 hours. After that 5 mL H_2O were added to the mixture and then extracted with $CHCl_3$ (30 mL). The organic layer was dried with $MgSO_4$ and concentrated in vacuo. The residue was purified by column chromatography on silica using $CHCl_3$/CH_3OH (v/v, 99/5) as an eluent mixture to afford **2**, **4** and **6** as yellow solids and **5** as a yellow oil.

Fluorescent probe 2: Yield 38% (76 mg); M.p.: 76 °C (decomp.); ^1H NMR (CDCl$_3$, 300 MHz): $\delta = 8.74$ (s, 1 H), 8.37 (d, $J = 5.7$ Hz, 1 H), 7.47 (s, 1 H), 7.38 (d, $J = 7.7$ Hz, 1 H), 7.13 (d, $J = 5.9$ Hz, 2 H), 6.44 (s, 1 H), 3.93 (s, 3 H), 3.68 (m, 20 H), 3.44–3.39 (m, 2 H), 3.02 (s, 3 H), 2.82–2.76 (m, 2 H), 2.02–1.94 ppm (m, 2 H); ^{13}C NMR (CDCl$_3$, 75 MHz): $\delta = 157.2$, 154.8, 152.8, 150.6, 134.5, 129.1, 127.7, 121.4, 119.9, 118.5, 116.9, 109.4, 107.3, 98.6, 96.1, 71.1, 71.0, 70.6, 70.3, 70.2, 55.9, 53.1, 51.1, 39.2, 27.4, 21.6 ppm; HRMS (ESI): m/z calcd for $C_{32}H_{39}N_5O_7+H^+$: 606.2922 $[M+H^+]$; found: 606.2928.

Fluorescent probe 4: Yield 55% (115 mg); M.p.: 123 °C (decomp.); ^1H NMR (CDCl$_3$, 300 MHz): $\delta = 8.70$ (s, 1 H), 8.43 (s, 1 H), 7.49–7.38 (m, 2 H), 7.37–7.31 (m, 1 H), 7.10 (d, $J = 8.0$ Hz, 1 H), 6.68 (dd, $J = 8.9$, 2.2 Hz, 1 H), 6.56 (d, $J = 2.0$ Hz, 1 H), 4.72 (dt, $J = 11.9$, 5.9 Hz, 1 H), 3.80–3.60 (m, 16 H), 3.52–3.42 (m, 8 H), 1.37 (d, $J = 6.0$ Hz, 6 H), 1.24 ppm (t, $J = 7.0$ Hz, 6 H); ^{13}C NMR (CDCl$_3$, 75 MHz): $\delta = 157.0$, 156.0, 151.9, 148.1, 134.3, 130.1, 121.6, 121.2, 119.8, 118.9, 117.7, 113.4, 110.3, 107.6, 97.5, 71.3, 70.9, 70.7, 70.6, 70.5, 53.7, 45.2, 22.5, 12.6 ppm; HRMS (ESI): m/z calcd for $C_{34}H_{45}N_5O_7+H^+$: 636.3397 $[M+H^+]$; found: 636.3382.

Fluorescent probe 5: Yield 20% (42 mg); ^1H NMR (CDCl$_3$, 300 MHz): $\delta = 8.71$ (s, 1 H), 8.37 (s, 1 H), 7.46 (s, 1 H), 7.34 (dd, $J = 8.2$, 1.4 Hz, 1 H), 7.11 (s, 2 H), 6.44 (s, 1 H), 4.72 (dt, $J = 11.8$, 5.8 Hz, 1 H), 3.75–3.59 (m, 16 H), 3.51 (s, 4 H), 3.44–3.38 (m, 2 H), 3.01 (s, 3 H), 2.79 (t, $J = 6.1$ Hz, 2 H), 2.04–1.93 (m, 2 H), 1.38 ppm (d, $J = 6.0$ Hz, 6 H); ^{13}C NMR (CDCl$_3$, 75 MHz): $\delta = 157.1$, 154.8, 150.5, 147.8, 134.4, 128.9, 127.7, 121.4, 119.8, 118.6, 117.0, 112.7, 107.3, 96.1, 71.1, 71.0, 70.7, 70.6, 70.5, 53.5, 51.1, 39.2, 27.4, 22.4, 21.6 ppm; HRMS (ESI): m/z calcd for $C_{34}H_{43}N_5O_7+H^+$: 634.3241 $[M+H^+]$; found: 634.3225.

Fluorescent probe 6: Yield 58% (126 mg); M.p.: 165 °C (decomp.); ^1H NMR (CDCl$_3$, 600 MHz): $\delta = 8.69$ (s, 1 H), 8.34 (s, 1 H), 7.46 (s, 1 H), 7.34 (d, $J = 8.1$ Hz, 1 H), 7.09 (d, $J = 7.6$ Hz, 1 H), 7.00 (s, 1 H), 4.76–4.68 (m, 1 H), 3.70–3.65 (m, 16 H), 3.51 (s, 4 H), 3.33–3.31 (m, 4 H), 2.93 (t, $J = 6.4$ Hz, 2 H), 2.79 (t, $J = 6.1$ Hz, 2 H), 1.99 (dt, $J = 18.7$, 6.2 Hz, 4 H), 1.37 ppm (d, $J = 6.0$ Hz, 6 H); ^{13}C NMR (CDCl$_3$, 125 MHz): $\delta = 157.3$, 150.9, 150.7, 147.9, 147.0, 141.3, 134.9, 126.0, 123.8, 120.7, 119.9, 119.6, 118.5, 116.2, 112.6, 107.2, 106.3, 71.0, 70.7, 70.6, 70.4, 70.3, 53.4, 50.2, 49.8, 27.6, 22.3, 21.7, 20.3 ppm; HRMS (ESI): m/z calcd for $C_{36}H_{45}N_5O_7+H^+$: 660.3397 $[M+H^+]$; found: 660.3380.

CuACC procedure for 10: A mixture of the azido substituted crown compound **17c** (0.329 mmol) and 3-ethynyl-7-diethylcoumarin[12b] (cf. Scheme 4) (0.329 mmol), $CuSO_4 \cdot 5H_2O$ (4.1 mg) and sodium ascorbate (6.5 mg) in 9 mL THF/H_2O (v/v, 2/1) was stirred at 60 °C for 48 hours. After that 5 mL H_2O were added to the mixture and then extracted with $CHCl_3$ (30 mL). The organic layer was dried with $MgSO_4$ and concentrated in vacuo. The residue was purified by column chromatography on silica using $CHCl_3$/CH_3OH (v/v, 99/5) as an eluent mixture to afford **10** as a yellow solid.

Fluorescent probe 10: Yield 33% (71 mg); M.p.: 88 °C (decomp.); ^1H NMR (CDCl$_3$, 600 MHz): $\delta = 8.72–8.67$ (m, 2 H), 7.46–7.42 (m, 2 H), 7.23 (m, 2 H), 6.65 (dd, $J = 8.9$, 2.2 Hz, 1 H), 6.56 (d, $J = 2.2$ Hz, 1 H), 4.30–3.30 (m, 31 H), 1.24 ppm (t, $J = 7.1$ Hz, 6 H); HRMS (ESI): m/z calcd for $C_{34}H_{45}N_5O_8+H^+$: 652.3346 $[M+H^+]$; found: 652.3375.

General CuACC procedure for 7, 8 and 9: A mixture of the corresponding azido substituted crown compound **17a** or **17b** (0.415 mmol) and the corresponding alkynyl substituted fluorophore derivative[10] (cf. Scheme 4) (0.415 mmol), $CuSO_4 \cdot 5H_2O$ (5.3 mg) and sodium ascorbate (8.2 mg) in 9 mL DMF/H_2O (v/v, 2/1) was stirred at 60 °C for 48 hours. After that 5 mL H_2O were added to the mixture and then extracted with $CHCl_3$ (30 mL). The organic layer was dried with $MgSO_4$ and concentrated in vacuo. The residue was purified by column chromatography on silica using $CHCl_3$/CH_3OH (v/v, 99/5) as an eluent mixture to afford **7**, **8** and **9** as yellow oils.

Fluorescent probe 7: Yield 30% (99 mg); ^1H NMR (CDCl$_3$, 300 MHz): $\delta = 7.94$ (s, 1 H), 7.09 (s, 2 H), 6.81–6.71 (m, 1 H), 6.63 (t, $J = 4.8$ Hz, 1 H), 6.08 (dd, $J = 6.2$, 0.9 Hz, 2 H), 4.67–4.55 (m, 3 H), 4.33 (q, $J = 7.1$ Hz, 4 H), 3.77–3.46 (m, 20 H), 2.97 (d, $J = 4.9$ Hz, 2 H), 1.41–1.28 ppm (m, 12 H); ^{13}C NMR (CDCl$_3$, 75 MHz): $\delta = 166.6$, 161.6, 150.9, 144.8, 141.9, 141.0, 130.8, 120.7, 112.5, 110.5, 107.8, 103.1, 102.9, 71.0, 70.5, 70.4, 70.3, 61.6, 53.2, 42.0, 35.3, 30.0, 22.0, 14.2 ppm; HRMS (ESI): m/z calcd for $C_{38}H_{49}N_5O_{14}+H^+$: 800.3354 $[M+H^+]$; found: 800.3328.

Fluorescent probe 8: Yield 23% (74 mg); ^1H NMR (CDCl$_3$, 300 MHz): $\delta = 7.98$ (s, 1 H), 7.14 (s, 2 H), 6.97–6.81 (m, 1 H), 6.67–6.58 (m, 1 H), 6.07 (d, $J = 6.7$, Hz, 2 H), 4.62 (s, 2 H), 4.34 (q, $J = 6.6$ Hz, 4 H), 4.00–3.34 (m, 23 H), 2.98 (s, 2 H), 1.40–1.19 ppm (m, 6 H); ^{13}C NMR (CDCl$_3$, 75 MHz): $\delta = 166.6$, 161.6, 153.1, 144.9, 141.9, 141.0, 128.8, 120.8, 112.6, 110.6, 105.1, 103.2, 102.9, 70.9, 70.6, 70.4, 69.9, 61.6, 53.4, 42.0, 35.3, 29.6, 14.2 ppm; HRMS (ESI): m/z calcd for $C_{36}H_{45}N_5O_{14}+H^+$: 772.3041 $[M+H^+]$; found: 772.3033.

Fluorescent probe 9: Yield 19% (50 mg); ^{1}H NMR (CDCl$_3$, 300 MHz): $\delta = 8.78$ (s, 1H), 8.48–7.99 (m, 9H), 7.48 (s, 1H), 7.36–7.20 (m, 2H), 4.10–3.31 ppm (m, 23H); ^{13}C NMR (CDCl$_3$, 75 MHz): $\delta = 147.9$, 140.8, 131.4, 131.3, 130.9, 128.7, 128.2, 127.9, 127.3, 127.2, 126.1, 125.4, 125.1, 125.1, 125.0, 124.9, 124.8, 124.7, 123.8, 121.3, 120.4, 116.1, 112.7, 105.4, 71.0, 70.5, 70.3, 70.1, 56.0, 53.2 ppm; HRMS (ESI): m/z calcd for C$_{37}$H$_{40}$N$_4$O$_6$+H$^+$: 637.3026 [M+H$^+$]; found: 637.3050.

Conflict of interest

The authors declare no conflict of interest.

[1] a) E. Murphy, D. A. Eisner, *Circ. Res.* **2009**, *104*, 292–303; b) D. M. Bers, W. H. Barry, S. Despa, *Cardiovasc. Res.* **2003**, *57*, 897–912.

[2] a) A. P. de Silva, H. Q. N. Gunaratne, T. Gunnlaugsson, M. Nieuwenhuizen, *Chem. Commun.* **1996**, 1967–1968; b) M. K. Kim, C. S. Lim, J. T. Hong, J. H. Han, H.-Y. Jang, H. M. Kim, B. R. Cho, *Angew. Chem. Int. Ed.* **2010**, *49*, 364–367; *Angew. Chem.* **2010**, *122*, 374–377; c) A. R. Sarkar, C. H. Heo, M. Y. Park, H. W. Lee, H. M. Kim, *Chem. Commun.* **2014**, *50*, 1309–1312; d) H. He, M. A. Mortellaro, M. J. P. Leiner, S. T. Young, Ro. J. Fraatz, J. K. Tusa, *Anal. Chem.* **2003**, *75*, 549–555; e) V. V. Martin, A. Rothe, K. R. Gee, *Bioorg. Med. Chem. Lett.* **2005**, *15*, 1851–1855; f) V. V. Martin, A. Rothe, Z. Diwu, K. R. Gee, *Bioorg. Med. Chem. Lett.* **2004**, *14*, 5313–5316; g) F. V. Englich, T. C. Foo, A. C. Richardson, H. Ebendorff-Heidepriem, C. J. Sumby, T. M. Monro, *Sensors* **2011**, *11*, 9560–9572; h) S. Uchiyama, E. Fukatsu, G. D. McClean, A. P. de Silva, *Angew. Chem. Int. Ed.* **2016**, *55*, 768–771; *Angew. Chem.* **2016**, *128*, 778–781.

[3] Selected review articles: a) J. F. Callan, A. P. de Silva, D. C. Magri, *Tetrahedron* **2005**, *61*, 8551–8588; b) B. Daly, J. Ling, A. P. de Silva, *Chem. Soc. Rev.* **2015**, *44*, 4203–4211; c) A. P. de Silva, H. Q. N. Gunaratne, T. Gunnlaugsson, A. J. M. Huxley, C. P. McCoy, J. T. Rademacher, T. E. Rice, *Chem. Rev.* **1997**, *97*, 1515–1566; d) J. Li, D. Yim, W.-D. Jang, J. Yoon, *Chem. Soc. Rev.* **2017**, *46*, 2437–2458.

[4] a) A. Minta, R. Y. Tsien, *J. Biol. Chem.* **1989**, *264*, 19449–19457; b) N. B. Sankaran, S. Nishizawa, M. Watanabe, T. Uchida, N. Teramae, *J. Mater. Chem.* **2005**, *15*, 2755–2761; c) S. Nishizawa, M. Watanabe, T. Uchida, N. Teramae, *J. Chem. Soc. Perkin Trans. 2* **1999**, 141–144; d) M. Taki, H. Ogasawara, H. Osaki, A. Fukazawa, Y. Sato, K. Ogasawara, T. Higashiyama, S. Yamaguchi, *Chem. Commun.* **2015**, *51*, 11880–11883.

[5] a) H. Szmacinski, J. R. Lakowicz, *Anal. Biochem.* **1997**, *250*, 131–138; b) S. Despa, J. Vecer, P. Steels, M. Ameloot, *Anal. Biochem.* **2000**, *281*, 159–17; c) P. Roder, C. Hille, *Photochem. Photobiol. Sci.* **2014**, *13*, 1699–1710; d) T. Schwarze, H. Müller, S. Ast, D. Steinbrück, S. Eidner, F. Geißler, M. U. Kumke, H.-J. Holdt, *Chem. Commun.* **2014**, *50*, 14167–14170.

[6] a) V. V. Rostovtsev, L. G. Green, V. V. Folkin, K. B. Sharpless, *Angew. Chem. Int. Ed.* **2002**, *41*, 2596–2599; *Angew. Chem.* **2002**, *114*, 2708–2711; b) C. W. Tornøe, C. Christensen, M. Meldal, *J. Org. Chem.* **2002**, *67*, 3057–3062.

[7] a) S. Ast, H. Müller, R. Flehr, T. Klamroth, B. Walz, H.-J. Holdt, *Chem. Commun.* **2011**, *47*, 4685–4687; b) S. Ast, T. Schwarze, H. Müller, A. Sukhanov, S. Michaelis, J. Wegener, O. S. Wolfbeis, T. Körzdörfer, A. Dürkop, H.-J. Holdt, *Chem. Eur. J.* **2013**, *19*, 14911–14917; c) T. Schwarze, R. Schneider, J. Riemer, H.-J. Holdt, *Chem. Asian J.* **2016**, *11*, 241–247; d) T. Schwarze, J. Riemer, S. Eidner, H.-J. Holdt, *Chem. Eur. J.* **2015**, *21*, 11306–11310; e) T. Schwarze, M. Mertens, P. Müller, J. Riemer, P. Wessig, H.-J. Holdt, *Chem. Eur. J.* **2017**, *23*, 17186–17190; f) T. Schwarze, J. Riemer, H.-J. Holdt, *Chem. Eur. J.* **2018**, *24*, 10116–10121.

[8] T. Schwarze, H. Müller, D. Schmidt, J. Riemer, H.-J. Holdt, *Chem. Eur. J.* **2017**, *23*, 7255–7263.

[9] a) G. Jones II, W. R. Jackson, A. M. Halpern, *Chem. Phys. Lett.* **1980**, *72*, 391–395; b) G. Jones II, W. R. Jackson, C.-Y. Choi, *J. Phys. Chem.* **1985**, *89*, 294–300.

[10] R. Wawrzinek, J. Ziomkowska, J. Heuveling, M. Mertens, A. Herrmann, E. Schneider, P. Wessig, *Chem. Eur. J.* **2013**, *19*, 17349–17357.

[11] a) S. Müller, B. Liepold, G. J. Roth, H. J. Bestmann, *Synlett* **1996**, 521–522; b) S. Ohira, *Synth. Commun.* **1989**, *19*, 561–564.

[12] a) K. Sivakumar, F. Xie, B. M. Cash, S. Long, H. N. Barnhill, Q. Wang, *Org. Lett.* **2004**, *6*, 4603–4606; b) D.-N. Lee, G.-J. Kim, H.-J. Kim, *Tetrahedron Lett.* **2009**, *50*, 4766–4768.

[13] For detailed experimental data see Supporting Information.

[14] T. Gunnlaugsson, H. Q. N. Gunaratne, M. Nieuwenhuyzen, J. P. Leonard, *J. Chem. Soc. Perkin Trans. 1* **2002**, 1954–1962.